Molecular basis of R-type calcium channels in central amygdala neurons of the mouse

Seung-Chan Lee*, Sukwoo Choi†‡, Taehoon Lee§, Hyung-Lae Kim¶, Hemin Chin‖, and Hee-Sup Shin*‡

*National Creative Research Initiatives Center for Calcium and Learning, Korea Institute of Science and Technology, Seoul 136-791, Korea; †Department of Neuroscience, Ewha Institute of Neuroscience, Ewha Womans University, Ewha Medical Center, Seoul 110-783, Korea; §Department of Life Science, Pohang University of Science and Technology, Pohang 790-784, Korea; ¶Department of Biochemistry, Medical College, Ewha Womans University, Seoul 158-710, Korea; and ‖Genetics Research Branch, Division of Neuroscience and Basic Behavioral Science, National Institutes of Health, Bethesda, MD 20892

Communicated by Richard W. Tsien, Stanford University School of Medicine, Stanford, CA, December 26, 2001 (received for review November 19, 2001)

R-type Ca^{2+} channels play a critical role in coupling excitability to dendritic Ca^{2+} influx and neuronal secretion. Unlike other types of voltage-sensitive Ca^{2+} channels (L, N, P/Q, and T type), the molecular basis for the R-type Ca^{2+} channel is still unclear, thereby limiting further detailed analyses of R-type Ca^{2+} channel physiology. The prevailing hypothesis is that α_{1E} ($Ca_V2.3$) gene encodes for R-type Ca^{2+} channels, but the dearth of critical evidence has rendered this hypothesis controversial. Here we generated α_{1E}-deficient mice ($\alpha_{1E}-/-$) and examined the status of voltage-sensitive Ca^{2+} currents in central amygdala (CeA) neurons that exhibit abundant α_{1E} expression and R-type Ca^{2+} currents. The majority of R-type currents in CeA neurons were eliminated in $\alpha_{1E}-/-$ mice whereas other Ca^{2+} channel types were unaffected. These data clearly indicate that the expression of α_{1E} gene underlies R-type Ca^{2+} channels in CeA neurons. Furthermore, the $\alpha_{1E}-/-$ mice exhibited signs of enhanced fear as evidenced by their vigorous escaping behavior and aversion to open-field conditions. These latter findings imply a possible role of α_{1E}-based R-type Ca^{2+} currents in amygdala physiology associated with fear.

Voltage-sensitive Ca^{2+} channels, classified into L, N, P/Q, R, and T types, are critical for coupling excitability to Ca^{2+}-dependent processes within neurons and excitable cells (1). Whereas much has been learned about L, N, P/Q, and T types, the importance of R-type Ca^{2+} channels, originally defined as a channel "resistant" to blockers for L-, N-, and P/Q-type Ca^{2+} channels, has not been revealed up until recently. The R-type Ca^{2+} channel has been suggested to play a critical role in the release of neurotransmitters (2–5) and to be the major source of dendritic Ca^{2+} influx in response to action potentials (6–8). Thus, R-type Ca^{2+} channels appear to be a key component in controlling neural functions.

The identification of $\alpha 1$ subunit for each Ca^{2+} channel has been very critical for understanding Ca^{2+} channel physiology, and $\alpha 1$ subunits for L, N, P/Q, and T types have been successfully documented mainly because of the availability of a number of drugs and toxins that selectively target corresponding $\alpha 1$ subunits. Although the matching of R-type channel to $\alpha 1$ subunit is perhaps the main outstanding issue in the whole Ca^{2+} channel field, it has been difficult to characterize the corresponding $\alpha 1$ subunit for R-type Ca^{2+} channels mainly because of the lack of selective antagonists for the R-type channel currents (9).

It has been hypothesized that R-type Ca^{2+} currents result from the expression of the α_{1E} gene (10–12). Antisense knockout of the α_{1E} subunit in cerebellar granule neurons produced a partial reduction in R-type Ca^{2+} currents, in good agreement with this hypothesis (13, 14). However, a toxin (SNX-482) that selectively blocked the α_{1E}–based Ca^{2+} currents in heterologous expression systems failed to block R-type Ca^{2+} currents in several instances, including cerebellar granule neurons (9, 14). Even more confusion has been introduced to this controversial subject by a recent study using α_{1E}-deficient mice. This particular study has suggested that the majority of R-type Ca^{2+} currents in cerebellar granule neurons do not result from the expression of α_{1E} (15). Thus, experiments using different methods give rise to contradictory results in cerebellar granule cells, rendering the molecular nature of R-type Ca^{2+} channels elusive.

In the present study, we provide clear-cut evidence that complete deletion of α_{1E} specifically eliminates the majority of R-type components of Ca^{2+} currents in central amygdala (CeA) neurons, strongly supporting the hypothesis that R-type channels are encoded by α_{1E}. Furthermore, we present behavioral data that provides insight into the function of α_{1E}-based R-type channel currents in the CeA.

Materials and Methods

Generation of $\alpha_{1E}-/-$ Mice. A 24.9-kb genomic DNA fragment containing the exon including the first translated region with the initiation codon of the α_{1E} locus was isolated from a 129/svJae mouse genomic library by screening with the 476-bp (nucleotides 100–575) rat α_{1E} cDNA probe. We designed a targeting vector to replace the 0.5-kb *Xba*I–*Cla*I fragment within the exon (from nucleotide 357 to 860 of mouse α_{1E} cDNA) including the initiation codon and a part of the N-terminus cytosolic domain with a fragment containing the green fluorescent protein (GFP) gene and the neo cassette [phosphoglycerol kinase (PGK) promoter-neo-PGK poly(A)] to induce gene disruption and facilitate positive selection (Fig. 1*A*). As a result, the GFP and neo cassette is flanked by a 6.1-kb *Sal*I–*Xba*I fragment and a 3.1-kb *Cla*I–*Sma*I fragment as 3′ and 5′ homologous regions, respectively. For a negative selection, the thymidine kinase cassette [PGK promoter–herpes simplex virus thymidine kinase–PGK poly(A)] was attached at the 5′ end of the 5′ homology region. Embryonic stem (ES) cell cultures and embryo manipulations were performed as described (16, 17). J1 ES cells were electroporated with the linearized targeting vector, and the positive clones were identified by Southern blotting analysis of *Apa*I/*Spe*I-digested genomic DNA. The 0.8-kb *Sma*I–*Xho*I fragment in the 5′ flanking region was used as the probe for Southern blotting analysis (Fig. 1*A*). ES clones harboring the desired homologous recombination were injected into C57BL/6J host blastocysts to generate chimeras. Germ-line-competent male chimeras were bred with C57BL/6J females to produce heterozygous mice (F_1). Western blot analysis was used to confirm the lack of the α_{1E} protein in the mutant by using rabbit polyclonal anti-α_{1E} antibodies (Alomone Laboratories, Jerusalem).

Animals. To establish parental strains, F_1 $\alpha_{1E}+/-$ mice were backcrossed in parallel to C57BL/6J or 129/svJae inbred mice for 3–4 generations. In all experiments, mice in mixed back-

Abbreviations: CeA, central amygdala; WC, whole-cell capacitance.

‡To whom reprint requests should be addressed. E-mail: shin@kist.re.kr or sukwoo@mm.ewha.ac.kr.

The publication costs of this article were defrayed in part by page charge payment. This article must therefore be hereby marked "*advertisement*" in accordance with 18 U.S.C. §1734 solely to indicate this fact.

www.pnas.org/cgi/doi/10.1073/pnas.052697799

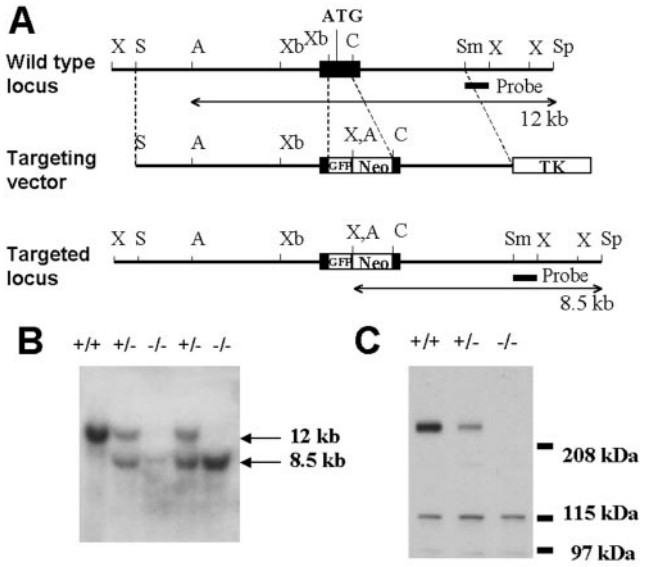

Fig. 1. Generation of $\alpha_{1E}-/-$ mice. (*A*) Structure and simplified restriction maps of the wild-type locus (*Top*), the targeting vector (*Middle*), and the disrupted locus (*Bottom*) of the α_{1E} gene. The exon containing the first translated region of the α_{1E} gene is boxed. Double-arrowhead lines under the wild type, and the targeted locus represent the expected fragments (12 kb for the wild type and 8.5 kb for the mutant) after digestion with *Apa*I/*Spe*I and hybridization with the probe (the closed box under the two loci). Restriction sites: A, *Apa*I; C, *Cla*I; S, *Sal*I; Sm, *Sma*I; Sp, *Spe*I; X, *Xho*I; Xb, *Xba*I. GFP, green fluorescent protein; TK, thymidine kinase. (*B*) Southern analysis of tail DNA from wild-type, heterozygous, and homozygous mutant mice. Genomic DNA was digested with *Apa*I/*Spe*I, transferred to a nylon membrane, and hybridized with the ^{32}P-labeled probe. +/+, wild type; +/−, heterozygote; −/−, homozygote. (*C*) Western blot analysis of brain membrane fractions from wild-type, heterozygous, and homozygous mutant mice. The band around 260 kDa, the predicted size of α_{1E} protein, is specifically absent in the homozygous mutant.

grounds obtained from these parental strains of C57BL/6J (N3–4) $\alpha_{1E}+/-$ or 129/svJae (N3–4) $\alpha_{1E}+/-$ mice were used. In voltage-dependence experiments and toxin mixture treatment experiments, mice obtained from crossings of C57BL/6J(N3–4) × C57BL/6J (N3–4) or C57BL/6J (N3–4) × 129/svJae (N3–4) were used. In serial toxin treatment experiments, mice obtained from crossings of C57BL/6J (N3–4) × 129/svJae (N3–4) were used. In behavioral experiments, mice obtained from crossings of C57BL/6J(N4) × C57BL/6J(N4) were used. Age-matched littermates were used as controls in all experiments. Animals were subjected to a 12-h light/dark cycle, with free access to food and water. Animal care and handling was carried out according to the guidelines of the institute.

Preparation of Acutely Dissociated CeA Neurons. The acutely dissociated CeA neurons were prepared as described (18) from 15- to 25-day-old pups. Brains were cooled rapidly in a dissecting solution containing 120 mM NaCl, 10 mM KCl, 2 mM KH_2PO_4, 1 mM $CaCl_2$, 6 mM $MgSO_4$, 10 mM d-glucose, and 10 mM piperazine-*N*,*N*-bis-[2-ethanesulfonic acid] (pH adjusted to 7.3–7.4) through which 100% O_2 was continuously bubbled at 0–5°C. The osmolarity of the dissecting solution was adjusted to 300–310 mOsM with sucrose. Transverse amygdala slices (250 or 300-μm) were sectioned by using a vibratome (Technical Products International, St. Louis) in the cold dissecting solution followed by preincubation in the oxygenated dissecting solution for 20–30 min at room temperature. The slices were then incubated for 10–12 min in the dissecting solution containing pronase E (10–15 mg, 4 units/mg, type XIV, Sigma) and trypsin (7–10 mg, 9 *N*-benzoyl-L-arginine ethyl ester units/mg, type XI, Sigma), oxygenated at 34.5°C. The slices were then washed twice and placed in the oxygenated dissecting solution at room temperature for another 10 min. Subsequently, the CeA was carefully removed by dissection and triturated gently to dissociate the individual neurons. Healthy-looking neurons of round, oval, or pyramidal shapes were used for patch-clamp recording.

Whole-Cell Patch-Clamp Recording. Whole-cell patch-clamp experiments were carried out as described (19–22). Patch electrodes were made from borosilicate capillary tubes (1.2 mm OD, standard wall, Warner Instruments, Hamden, CA), pulled with a micropipette puller (model P-87, Sutter Instruments, Novato, CA), and polished with a microforge (MF-9, Narishige, Tokyo). The patch electrodes had a resistance of 2.5–4 MΩ when filled with an internal solution composed of 90 mM cesium acetate, 18 mM tetraethylammonium chloride, 18 mM *N*-[2-hydroxyethyl]piperazine-*N*-[2-ethanesulfonic acid], 9 mM 1,2-bis(2-aminophenoxy)ethane-*N*,*N*,*N*,*N*-tetraacetic acid, 9 mM D-glucose, 5 mM Mg-ATP, 0.2 mM sodium guanosine 5-triphosphate, and 0.1 mM leupeptin, pH adjusted to 7.1–7.2 with 1 M CsOH at room temperature, final osmolarity of 270–280 mOsM. The external solution consisted of 120 mM tetraethylammonium chloride, 3 mM $CaCl_2$, 10 mM *N*-[2-hydroxyethyl]piperazine-*N*-[2-ethanesulfonic acid], 10 mM CsCl, 5 mM 4-aminopyridine, 10 mM D-glucose, and 1 μM tetrodotoxin. The pH of the external solution was titrated to ≈7.4 with 1 M HCl or 1 M CsOH, and the osmolarity was adjusted to 320 ± 5 mOsM with sucrose. Currents were recorded by using the Axopatch 200B amplifier, filtered at 1 or 2 kHz by a built-in filter, and stored in the computer. Leak corrections were performed by using a P/4 trace subtraction. The series resistance (<20 MΩ) was compensated >50%. Recordings exhibiting >30% change in series resistance were discarded whereas junction potentials were not corrected. Command pulses were delivered at 15- or 30-s intervals from −70 mV to 10 mV to elicit Ca^{2+} currents. To examine the voltage dependence of Ca^{2+} currents, a series of command pulses (−50 to 50 mV) were delivered from a holding potential of −70 mV at 10-s intervals. All of the experiments were performed at room temperature (24–28°C). Data are expressed as means ± SE, and statistical comparisons were made by using the Student's *t* test.

Drug solutions were delivered by gravity feed (≈1 ml/min) from a linear array of glass capillaries. Nifedipine (Sigma) was prepared as a concentrated stock solution in DMSO and protected from light. ω-Conotoxin GVIA (Alomone Labs) was prepared as a concentrated stock in the external solution and stored in aliquots at −70°C. The stocks of drugs were diluted in the external solution just before each experiment. Cytochrome *c* (0.1 mg/ml) was included in all external solutions to block nonspecific binding of toxins.

Behavioral Analysis. Animals at the age of 7–12 weeks were used in behavioral studies with all animals being brought to the experimental room at least 1 h before the behavioral testing. Averaged values were compared statistically by *t* test (criterion for significance, $P < 0.05$), unless otherwise noted.

Rotarod test. The rotarod test was performed as described (20). Briefly, mice were placed in a neutral position on a stationary 3-cm diameter cylinder of the rotarod apparatus (Letica Scientific Instruments, Barcelona). Rotation was initiated and gradually increased from 4 to 35 rpm over the course of 5 min. Latency to fall was recorded for each mouse in three trials with 20-min intervals between trials. The rotarod test was performed between 11 a.m. and 4 p.m.

Open-field test. The open field (23) was made of white plastic plate and was 40 cm long × 40 cm wide × 37 cm high in size. The light intensity on the central platform was 40 lux. Each mouse

was transferred to the periphery of the field, and the total horizontal distance moved and the time spent in the central area were measured for 5 min by using a video tracking system (HVS Image, Buckingham, U.K.). A computer program was used to overlay grid lines that divided the open field into 16 square regions. The inner four square regions were defined as the central area. The open-field test was performed between 11 a.m. and 4 p.m.

Elevated plus maze. The elevated plus maze (24) consisted of two open arms (25 cm × 8 cm) and two closed arms with a 15-cm high wall arranged such that arms of the same type were opposite each other with arms being connected by an open central area. The light intensity on the central platform was 20 lux. All parts of the apparatus were made of black plastic plate, and the maze was placed at a height of 50 cm from the floor. Each mouse was transferred to the closed arm facing the central area and was allowed to explore freely for 5 min. The amount of time spent in the open and closed arms was measured. The elevated plus maze was performed during the early dark phase of light-dark cycles.

Results

Generation of $\alpha_{1E}-/-$ Mice. Homozygous $\alpha_{1E}-/-$ mice were obtained by mating heterozygotes. Wild-type, heterozygous, and homozygous mutant offspring were produced at the predicted Mendelian ratio (1:2:1). Homozygous mice were healthy and fertile and exhibited no gross phenotypic abnormality. To confirm the null mutation of the α_{1E} gene we performed Western blot analysis with wild-type, heterozygote, and homozygote mouse brains (Fig. 1*C*). Probing of membrane fractions of wild-type brain with anti-α_{1E} antibodies resulted in an intense band at around 260 kDa, which is the predicted size of the α_{1E} protein, together with additional weaker bands with molecular masses less than 130 kDa. The smaller bands are believed to be nonspecific, crossreactive bands. The 260-kDa band was specifically absent in membrane fractions of homozygous mutant brain as depicted in Fig. 1*C*. From this result, we conclude that a null mutation of α_{1E} was successfully produced by our targeting strategy.

Reduced R-Type Currents in the $\alpha_{1E}-/-$ CeA Neurons. Both mRNA and translated protein products of the α_{1E} gene are abundantly expressed in the amygdaloid complex (25–27). R-type currents comprise the largest component of total Ca^{2+} currents in the CeA neurons and resemble the general characteristics of α_{1E}-based currents defined in heterologous expression systems (18). To study the relationship between the α_{1E} subunits and R-type currents we examined the properties of the voltage-sensitive Ca^{2+} currents in CeA neurons acutely dissociated from $\alpha_{1E}-/-$ mice and their wild-type littermates.

Fig. 2*A* illustrates a typical Ca^{2+} current elicited by step depolarizations to a wide range of voltages. In $\alpha_{1E}+/+$ neurons, the Ca^{2+} currents are normally activated at around −20 mV and peaked at around 10 mV. The current voltage relationship in $\alpha_{1E}-/-$ neurons was similar to that evident in $\alpha_{1E}+/+$ neurons, whereas the total current density in $\alpha_{1E}-/-$ neurons was significantly reduced at all testing voltages above −10 mV (Fig. 2*B*). Thus, the component of Ca^{2+} currents absent in $\alpha_{1E}-/-$ neurons appears to be the high voltage-activated type. This finding is consistent with a previous report in which α_{1E} encoded a high voltage-activated type channel in a heterologous expression system when Ca^{2+} ions were used as charge carriers (26, 28).

We have used two different protocols to estimate the proportion of R-type Ca^{2+} current in the neurons. In the first protocol, the simultaneous blockade of L-, N- and P/Q-type Ca^{2+} channels was achieved by applying a mixture of 10 μM nifedipine, 2 μM ω-conotoxin GVIA, and 0.4 μM ω-agatoxin IVA. In the second protocol, the successive application of specific blockers was performed including 10 μM nifedipine for L-type, 1 μM

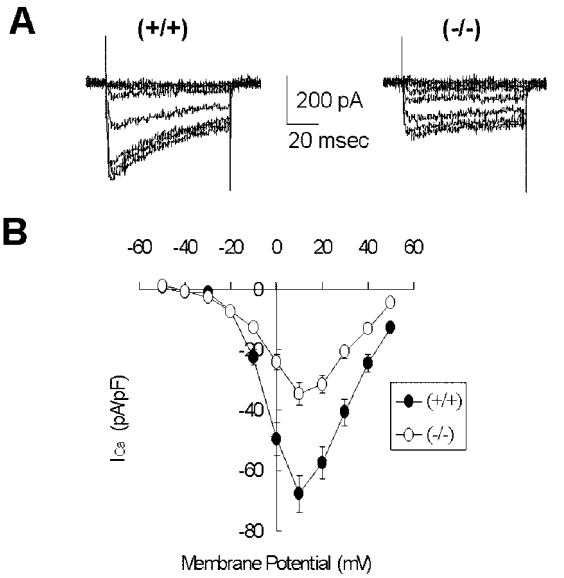

Fig. 2. Voltage dependence of the total Ca^{2+} current density in acutely dissociated CeA neurons. (*A*) Representative superimposed current traces of CeA neurons from $\alpha_{1E}+/+$ [*Left*, whole-cell capacitance (WC) = 5.5 pF] and $\alpha_{1E}-/-$ (*Right*, WC = 7 pF) mice are shown. Ca^{2+} currents were elicited by a series of voltage steps from −50 to +20 mV (with 10-mV increments) delivered at 10-s intervals with holding potential at −70 mV. (*B*) The current-voltage plot in both genotypes. Ca^{2+} currents were elicited by a series of voltage steps from −50 to +50 mV (with 10-mV increments) delivered at 10-s intervals with holding potential at −70 mV. ●, $\alpha_{1E}+/+$ (n = 17); ○, $\alpha_{1E}-/-$ (n = 12).

ω-conotoxin GVIA for N-type, and 0.4 μM ω-agatoxin IVA for P/Q-type Ca^{2+} channels. In response to the mixture treatment, the current density was reduced from 69.6 ± 8.9 pA/pF before treatment (n = 8) to 28.0 ± 3.9 pA/pF after treatment (n = 8) in $\alpha_{1E}+/+$ neurons. On the other hand, in $\alpha_{1E}-/-$ neurons, the current density was reduced from 45.3 ± 7.9 pA/pF before treatment (n = 6) to 5.5 ± 1.3 pA/pF after treatment (n = 6) (Fig. 3*A*). This result represents a decrease of the R-type current density in the mutant compared with the wild type by 81% ($P <$ 0.001). The experiments using serial blockers gave a comparable result to that obtained with the mixture treatment (Fig. 3*B*): the current density was reduced from 83.7 ± 7.2 pA/pF before treatment (n = 9) to 37.1 ± 3.1 pA/pF after treatment (n = 5) in $\alpha_{1E}+/+$ neurons, whereas, in $\alpha_{1E}-/-$ neurons, the current density was reduced from 46.2 ± 7.4 pA/pF before treatment (n = 15) to 4.6 ± 0.96 pA/pF after treatment (n = 10), a decrease of 88% in the R-type current density in the mutant compared with the wild type ($P <$ 0.0001). When the data from both protocols were pooled together, total current density was decreased from 77.0 ± 5.7 pA/pF (n = 17) in $\alpha_{1E}+/+$ to 46.0 ± 5.7 pA/pF (n = 21) in $\alpha_{1E}-/-$ neurons ($P <$ 0.001), whereas the residual R-type component was reduced from 31.5 ± 2.9 pA/pF (n = 13) in $\alpha_{1E}+/+$ to 4.9 ± 0.7 pA/pF (n = 16) in $\alpha_{1E}-/-$ neurons, a decrease of 84% ($P <$ 0.0001) (Fig. 3*C*). Therefore, the reduction in the R-type component accounted for a majority of the reduction in the total current density, suggesting that α_{1E} is responsible for a majority of the R-type component in the CeA neurons. However, it should be noted that some current components, albeit very small, were resistant to the mixture of blockers in $\alpha_{1E}-/-$ neurons, which suggests the possibility that other Ca^{2+} channels may contribute to R-type currents (Fig. 3) (15).

In an effort to characterize the nature of α_{1E}-based R-type currents, we compared the inactivation kinetics of Ca^{2+} currents between $\alpha_{1E}+/+$ and $\alpha_{1E}-/-$ neurons. The inactivation kinet-

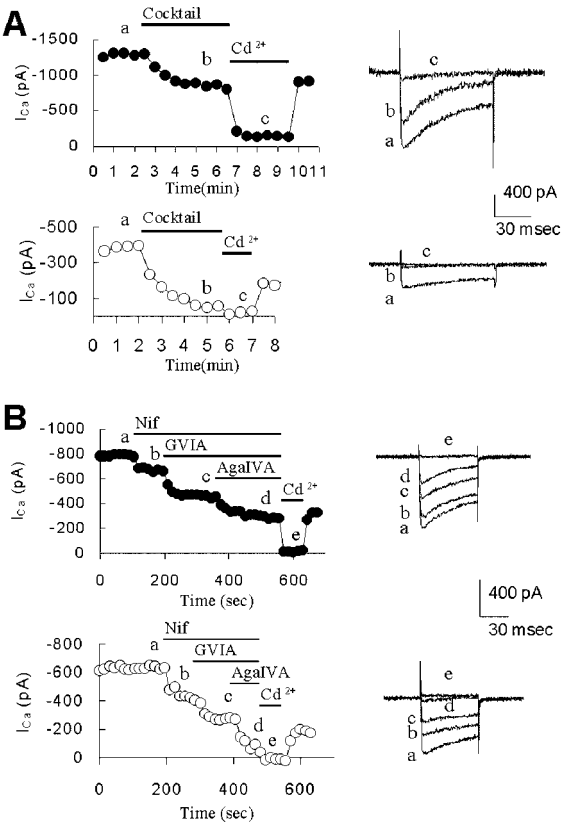

Fig. 3. Decreased total and R-type Ca^{2+} current densities in CeA neurons in $\alpha_{1E}-/-$ mice. (*A*) Analysis of currents using a mixture of blockers. Peak I_{Ca}, activated by 80 or 60 msec depolarization from −70 mV to 10 mV every 30 s, is plotted against time for an $\alpha_{1E}+/+$ neuron (WC = 17 pF) and an $\alpha_{1E}-/-$ neuron (WC = 9 pF). R-type Ca^{2+} current was isolated by application of a mixture consisting of 10 μM nifedipine, 2 μM ω-conotoxin GVIA, and 0.4 μM ω-agatoxin-IVA, and the Ca^{2+} current was identified by a final application of 200 μM Cd^{2+}. (*Right*) Examples of typical tracings are shown. (*Upper*) $\alpha_{1E}+/+$. (*Lower*) $\alpha_{1E}-/-$. CeA neurons of $\alpha_{1E}-/-$ exhibited a large reduction in the amount of R-type current density. (*B*) L-, N-, P/Q-, and R-type Ca^{2+} current of CeA neurons in $\alpha_{1E}+/+$ and $\alpha_{1E}-/-$ CeA neurons. Peak I_{Ca} activated by 60-msec depolarization from −70 mV to 10 mV every 15 s is plotted against time for an $\alpha_{1E}+/+$ neuron (WC = 8 pF) and an $\alpha_{1E}-/-$ neuron (WC = 18 pF). L-, N-, P/Q-, and R-type currents were blocked by serial applications of 10 μM nifedipine, 1 μM ω-conotoxin-GVIA, 0.4 μM ω-agatoxin-IVA, and 200 μM Cd^{2+}. (*Right*) Examples of typical tracings are shown. (*Upper*) $\alpha_{1E}+/+$. (*Lower*) $\alpha_{1E}-/-$. (*C*) Histogram of total and individual channel type current densities in $\alpha_{1E}+/+$ (filled bars), and $\alpha_{1E}-/-$ (empty bars) CeA neurons. Total current: $+/+$, $n = 15$; $-/-$, n =22; $P < 0.001$. L type: $+/+$, $n = 8$; $-/-$, $n = 14$; $P > 0.2$. N type: $+/+$, $n = 8$; $-/-$, $n = 14$; $P > 0.05$. P/Q type: $+/+$, $n = 7$; $-/-$, $n = 12$; $P > 0.9$. R type: $+/+$, $n = 13$; $-/-$, $n = 16$, $P < 0.0001$. It was noted that the proportion of R-type Ca^{2+} currents in $\alpha_{1E}+/+$ neurons exhibited some variation (around 50% of total Ca^{2+} current in 6/13 cells; around 30% of total Ca^{2+} current in 7/13 cells.). Data from the two groups of neurons were pooled to calculate R-type currents of the $\alpha_{1E}+/+$ neurons. Because the total and the R-type current density values were not significantly different between the mixture and the serial treatment protocols, results from both protocols were combined in this histogram.

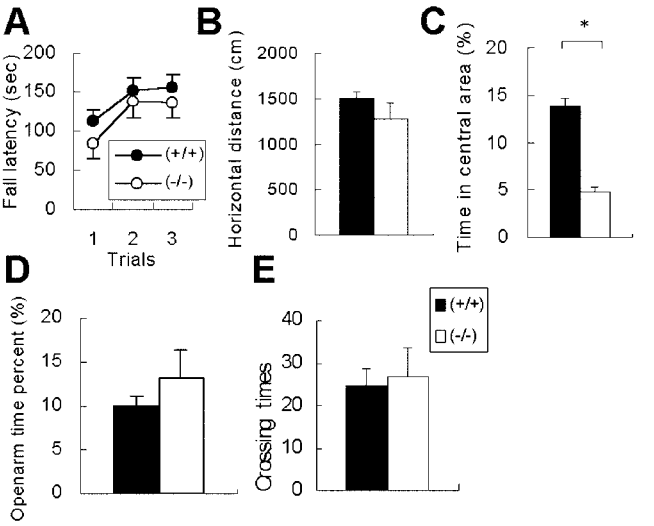

Fig. 4. Rotarod, open-field, and elevated plus maze tests. (*A*) Rotarod test. No significant difference was observed in the retention time on the rotating cylinder between $\alpha_{1E}+/+$ and $\alpha_{1E}-/-$ mice ($+/+$, $n = 13$; $-/-$, $n = 9$). (*B* and *C*) Open-field test. The total moving distance (*B*) and the percentage of time spent in the central area (*C*) were measured during the first 5 min after placing each mouse in the apparatus (filled bars, $+/+$, $n = 13$; empty bars, $-/-$, $n = 9$). The mutant mice spent significantly less time in the center area than the wild type. *, $P < 0.01$. (*D* and *E*) Elevated plus maze. The percentage of time spent in the open arms (*D*) and the total crossing number (*E*) were counted (filled bar: $+/+$, $n = 13$; empty bar: $-/-$, $n = 9$). No significant difference was found between $\alpha_{1E}+/+$ and $\alpha_{1E}-/-$ mice either in the open arms time or in the crossing number.

ics of total Ca^{2+} currents in $\alpha_{1E}+/+$ neurons was more rapid than that evident in $\alpha_{1E}-/-$ neurons ($+/+$: $\tau = 29.9 \pm 1.2$, $n = 17$; $-/-$: $\tau = 46.8 \pm 4.0$, $n = 21$; $P < 0.001$), indicating that the component absent in $\alpha_{1E}-/-$ neurons, supposedly R-type currents, has rapid inactivation kinetics. In fact, after a treatment with the blocker mixture the R-type currents in $\alpha_{1E}+/+$ neurons exhibited relatively rapid inactivation kinetics ($\tau = 24.1 \pm 1.1$, $n = 13$). These observations are consistent with the previous finding that α_{1E}-based Ca^{2+} channels exhibited relatively rapid inactivation kinetics in heterologous expression systems (25, 26, 29). This result reinforces the idea that the expression of α_{1E} underlies the majority of R-type currents.

The currents blocked by nifedipine or ω-agatoxin IVA were not significantly altered by deletion of α_{1E} (L type: $+/+$, 13.4 ± 0.8 pA/pF, $n = 8$, $-/-$, 15.2 ± 1.0 pA/pF, $n = 14$, $P > 0.2$; P/Q type: $+/+$, 21.1 ± 2.2 pA/pF, $n = 7$, $-/-$, 20.3 ± 7.5 pA/pF, $n = 12$, $P > 0.9$) (Fig. 3 *B* and *C*). Interestingly, the current component inhibited by ω-conotoxin GVIA appeared to be reduced from 14.9 ± 4.1 pA/pF ($n = 8$) in $\alpha_{1E}+/+$ to 7.8 ± 1.3 pA/pF ($n = 14$) in $\alpha_{1E}-/-$ neurons, but this difference did not reach statistical significance ($P > 0.05$) (Fig. 3 *B* and *C*).

In summary, the majority of R-type currents in CeA neurons were eliminated without a significant alteration of other high voltage-activated Ca^{2+} channels in α_{1E}-deficient mice.

Emotional Abnormality of $\alpha_{1E}-/-$ Mice. To examine the behavioral effect of impairment of R-type currents in CeA neurons, we explored the anxiety-related behavior of $\alpha_{1E}-/-$ mice, because the CeA is involved in the regulation of fear or stress-related behavior (30–32). $\alpha_{1E}-/-$ mice appeared normal with no significant motor defects evident in the rotarod test (Fig. 4*A*). However, $\alpha_{1E}-/-$ mice did exhibit some signs of fear or anxiety. They often showed vigorous escaping behavior during experimental handling. This escaping behavior of $\alpha_{1E}-/-$ mice was characterized by fast explosive runs from corner to corner of a

NEUROBIOLOGY

cage and was not observed in wild-type littermates. Mutant mice would occasionally jump out of the cage when the hand of an experimenter approached them. In the open-field test, the $\alpha_{1E}-/-$ mice spent significantly less time in the central area ($P < 0.01$) but there was no reduction of total locomotor activity, suggesting that the mutant had an increased anxiety level (Fig. 4 *B* and *C*). However, no significant differences were noted between wild-type and the $\alpha_{1E}-/-$ mice in the elevated plus maze assay (Fig. 4 *D* and *E*). The behavioral phenotypes of the $\alpha_{1E}-/-$ mice are generally consistent with those of a previous study (33) and are suggestive of a fear-related emotional abnormality in $\alpha_{1E}-/-$ mice.

Discussion

Our findings provide strong evidence that the α_{1E} subunit underlies R-type, toxin-resistant Ca^{2+} channel currents in CeA neurons and support the hypothesis that R-type Ca^{2+} channel currents result from the expression of the α_{1E} gene (10–12).

There has been much debate concerning the molecular nature of R-type Ca^{2+} channels (9, 15, 28). Experiments using antisense oligonucleotides to suppress α_{1E} expression generally support the idea that the α_{1E} gene encodes the Ca^{2+} channel subunit underlying R-type currents in cerebellar granule neurons (13, 14). In contrast, studies using either the SNX-482 toxin or genetic deletion of α_{1E} suggest that the majority of R-type Ca^{2+} channel currents did not result from the expression of α_{1E} in cerebellar granule neurons (9, 15). In particular, deletion of α_{1E} in cerebellar granule neurons did not significantly alter the total Ca^{2+} current density or the R-type current component, implying either the presence of heterogeneity in molecular components for R-type channel currents or some functional compensation by other Ca^{2+} channels in response to the α_{1E} deletion (15). By contrast, in the present study, genetic deletion of α_{1E} in CeA neurons produced a significant reduction of the total current density that was largely accounted for by a reduction of the R-type current density. These data provide an unequivocal example where complete deletion of α_{1E} specifically eliminates the majority of R-type, toxin-resistant components of Ca^{2+} currents.

The discrepancy between our results and the results by Wilson *et al.* (15) could be explained by the fact that the two labs used different concentrations of dihydropyridines to block L-type Ca^{2+} channels. Wilson *et al.* (15) used 500 nM nimodipine, whereas we used 10 μM nifedipine, a saturating concentration. Apparently, 500 nM nimodipine has been shown to be a subsaturating concentration to block L-type Ca^{2+} channel currents including α_{1D}-based currents (34). If subsaturating concentrations of the blocker are used, the R-type current will be contaminated with other Ca^{2+} currents and lead to an overestimation of the actual R-type component. Not surprisingly, in cerebellar granule neurons, the proportion of L-type Ca^{2+} current reported by Wilson *et al.* (15) is substantially smaller than that reported in the previous study using a saturating concentration of 10 μM nimodipine (19). Therefore, the use of a subsaturating concentration of nimodipine in the study of Wilson *et al.* (15) may cause incomplete blockade of L-type calcium channels, which could contribute to the presence of substantial, toxin-resistant components in $\alpha_{1E}-/-$ neurons.

It should be noted that in $\alpha_{1E}-/-$ CeA neurons some currents, albeit very small, were still resistant to the mixture of blockers for L, N, and P/Q channels in our experimental condition. As discussed in the previous section, such a resistant current component might have resulted from incomplete blockade of L-type calcium channel currents, especially α_{1D}-based currents, by dihydropyridines. α_{1D}-based currents in heterologous expression systems exhibited a very poor sensitivity to dihydropyridine (34, 35). In that study, only $\approx$50% of α_{1D}-based Ca^{2+} current was inhibited by 3 μM nimodipine, a saturating concentration (34). Consistent with this idea is a recent report that some of the R-type components in dorsal root ganglion neurons were blocked by very high concentrations of dihydropyridine, thereby implying that α_{1D}-based currents contribute to the R-type currents.** An alternative possibility is that the residual, toxin-resistant current in $\alpha_{1E}-/-$ neurons is caused by incomplete blockade of Q-type currents by the concentration of ω-agatoxin IVA used in our study (400 nM). This concentration of ω-agatoxin IVA has been shown to block around 90% of ω-agatoxin IVA-sensitive currents in cerebellar granule cells (11). Thus, the remaining, small fraction of the Q-type currents resistant to 400 nM ω-agatoxin IVA might contribute to the residual, toxin-resistant currents in $\alpha_{1E}-/-$ neurons.

Deletion of α_{1E} did not appear to alter the expression of other types of Ca^{2+} channels in CeA neurons, with the possible exception of N-type Ca^{2+} channels, which exhibited a slight, although not statistically significant, decrease in expression in α_{1E}-deficient mice. Recently the expression of N-type Ca^{2+} channels has been shown to change in proportion to total Ca^{2+} current density in superior cervical ganglion neurons (36), which may underlie the slightly diminished expression of N-type Ca^{2+} channels in α_{1E}-deficient neurons.

What is the functional relevance of α_{1E}-based, R-type Ca^{2+} channel currents in CeA neurons? In light of their prominent somatic and dendritic location (27), it is likely that R-type channel currents in CeA neurons are involved in the regulation of neuronal excitability. In fact, the blockade of Ca^{2+} channels dramatically increased neuronal excitability of CeA neurons and reduced afterhyperpolarization, suggesting that voltage-dependent Ca^{2+} channels regulate somatic and dendritic excitability through Ca^{2+}-activated K^+ channels (37). This notion also is supported by a recent study in which dendritic R-type Ca^{2+} channels were demonstrated to play a major role in mediating Ca^{2+} influx in response to action potentials (6–8). Because some CeA neurons ($\approx$40% of $\alpha_{1E}+/+$ CeA neurons) exhibit an extremely large amount of α_{1E}-based, R-type currents (see Fig. 3*A* and ref. 18), the modulation of R-type currents by other G protein-coupled neurotransmitter receptors (2, 38, 39) would be sufficient to regulate neuronal excitability in the CeA. The $\alpha_{1E}-/-$ mouse therefore will be a very useful tool to examine this question in the future.

The CeA is the major output structure of the amygdaloid complex and projects to brainstem and hypothalamic nuclei that are critically involved in fear responses (30–32). Electrical stimulation of the CeA induced fear-like responses (40–42), whereas lesions of the CeA reduced or completely blocked many autonomic, neuroendocrine, and behavioral responses evoked by unconditioned or conditioned fear-arousing stimuli (43–45). In this respect, the α_{1E}-deficient mice provided us with an opportunity to examine the relationship between R-type channel currents and amygdala-dependent behaviors. The $\alpha_{1E}-/-$ mice exhibited fear-related emotional abnormalities presumably as a result of enhanced neuronal activity in the CeA. As mentioned previously, loss of somatic and dendritic Ca^{2+} current density in α_{1E}-deficient mice could result in an increased excitability of the CeA (37), which in turn enhances the neuronal output of the whole amygdaloid complex. Thus, a deletion of α_{1E} would enhance fear-related behaviors through heightened outputs from the amygdaloid complex. Further physiological and behavioral analyses of the α_{1E}-deficient mice are merited in the future.

Oh, S. B., Monteil, A., Bhattacharyya, B., Ren, D. & Miller, R. J. (2001) *Soc. Neurosci. Abstr.* **31, no. 381.24.

We thank K. W. Lee for blastocyst injection, K. Jun for primary screening, J. L. Kim for help in embryonic stem cell culture, S. S. Choi for help in vector construction, Y. Namkung for help in patch-clamp recording, M. P. Kong for animal care, and S. W. Hong for help in genotyping. This work was supported by a grant from the National Creative Research Initiative Program, the Ministry of Science and Technology, Korea (to H.-S.S.), and Korea Ministry of Science and Technology Grant M1–0108-00–0051 under the neurobiology research program to S.C.

1. Tsien, R. W. & Wheeler, D. B. (1999) in *Calcium as a Cellular Regulator*, eds. Carafoli, E. & Klee, C. B. (Oxford Univ. Press, New York), pp. 171–199.
2. Wu, L. G., Borst, J. G. & Sakmann, B. (1998) *Proc. Natl. Acad. Sci. USA* **95,** 4720–4725.
3. Wu, L. G., Westenbroek, R. E., Borst, J. G., Catterall, W. A. & Sakmann, B. (1999) *J. Neurosci.* **19,** 726–736.
4. Wang, G., Dayanithi, G., Newcomb, R. & Lemos, J. R. (1999) *J. Neurosci.* **19,** 9235–9241.
5. Albillos, A., Neher, E. & Moser, T. (2000) *J. Neurosci.* **20,** 8323–8330.
6. Magee, J. C. & Johnston, D. (1995) *J. Physiol. (London)* **487,** 67–90.
7. Kavalali, E. T., Zhuo, M., Bito, H. & Tsien, R. W. (1997) *Neuron* **18,** 651–653.
8. Sabatini, B. L. & Svoboda, K. (2000) *Nature (London)* **408,** 589–593.
9. Newcomb, R., Szoke, B., Palma, A., Wang, G., Chen, X., Hopkins, W., Cong, R., Miller, J., Urge, L., Tarczy-Hornoch, K., *et al*. (1998) *Biochemistry* **37,** 15353–15362.
10. Zhang, J. F., Randall, A. D., Ellinor, P. T., Horne, W. A., Sather, W. A., Tanabe, T., Schwarz, T. L. & Tsien, R. W. (1993) *Neuropharmacology* **32,** 1075–1088.
11. Randall, A. & Tsien, R. W. (1995) *J. Neurosci.* **15,** 2995–3012.
12. Randall, A. D. & Tsien, R. W. (1997) *Neuropharmacology* **36,** 879–893.
13. Piedras-Renteria, E. S. & Tsien, R. W. (1998) *Proc. Natl. Acad. Sci. USA* **95,** 7760–7765.
14. Tottene, A., Volsen, S. & Pietrobon, D. (2000) *J. Neurosci.* **20,** 171–178.
15. Wilson, S. M., Toth, P. T., Oh, S. B., Gillard, S. E., Volsen, S., Ren, D., Philipson, L. H., Lee, E. C., Fletcher, C. F., Tessarollo, L., *et al*. (2000) *J. Neurosci.* **20,** 8566–8571.
16. Kim, D., Jun, K. S., Lee, S. B., Kang, N. G., Min, D. S., Kim, Y. H., Ryu, S. H., Suh, P. G. & Shin, H. S. (1997) *Nature (London)* **389,** 290–293.
17. Cho, C. H., Kim, S. S., Jeong, M. J., Lee, C. O. & Shin, H. S. (2000) *Mol. Cells* **10,** 712–722.
18. Yu, B. & Shinnick-Gallagher, P. (1997) *J. Neurophysiol.* **77,** 690–701.
19. Jun, K., Piedras-Renteria, E. S., Smith, S. M., Wheeler, D. B., Lee, S. B., Lee, T. G., Chin, H., Adams, M. E., Scheller, R. H., Tsien, R. W. & Shin, H. S. (1999) *Proc. Natl. Acad. Sci. USA* **96,** 15245–15250.
20. Kim, C., Jun, K., Lee, T., Kim, S. S., McEnery, M. W., Chin, H., Kim, H. L., Park, J. M., Kim, D. K., Jung, S. J., *et al*. (2001) *Mol. Cell. Neurosci.* **18,** 235–245.
21. Namkung, Y., Skrypnyk, N., Jeong, M. J., Lee, T., Lee, M. S., Kim, H. L., Chin, H., Suh, P. G., Kim, S. S. & Shin, H. S. (2001) *J. Clin. Invest.* **108,** 1015–1022.
22. Kim, D., Song, I., Keum, S., Lee, T., Jeong, M. J., Kim, S. S., McEnery, M. W. & Shin, H. S. (2001) *Neuron* **31,** 35–45.
23. Dulawa, S. C., Grandy, D. K., Low, M. J., Paulus, M. P. & Geyer, M. A. (1999) *J. Neurosci.* **19,** 9550–9556.
24. Pellow, S. & File, S. E. (1986) *Pharmacol. Biochem. Behav.* **24,** 525–529.
25. Soong, T. W., Stea, A., Hodson, C. D., Dubel, S. J., Vincent, S. R. & Snutch, T. P. (1993) *Science* **260,** 1133–1136.
26. Williams, M. E., Marubio, L. M., Deal, C. R., Hans, M., Brust, P. F., Philipson, L. H., Miller, R. J., Johnson, E. C., Harpold, M. M. & Ellis, S. B. (1994) *J. Biol. Chem.* **269,** 22347–22357.
27. Yokoyama, C. T., Westenbroek, R. E., Hell, J. W., Soong, T. W., Snutch, T. P. & Catterall, W. A. (1995) *J. Neurosci.* **15,** 6419–6432.
28. Bourinet, E., Zamponi, G. W., Stea, A., Soong, T. W., Lewis, B. A., Jones, L. P., Yue, D. T. & Snutch, T. P. (1996) *J. Neurosci.* **16,** 4983–4993.
29. Page, K. M., Stephens, G. J., Berrow, N. S. & Dolphin, A. C. (1997) *J. Neurosci.* **17,** 1330–1338.
30. LeDoux, J. E., Iwata, J., Cicchetti, P. & Reis, D. J. (1988) *J. Neurosci.* **8,** 2517–2529.
31. Davis, M. (1992) *Annu. Rev. Neurosci.* **15,** 353–375.
32. Applegate, C. D., Kapp, B. S., Underwood, M. D. & McNall, C. L. (1983) *Physiol. Behav.* **31,** 353–360.
33. Saegusa, H., Kurihara, T., Zong, S., Minowa, O., Kazuno, A., Han, W., Matsuda, Y., Yamanaka, H., Osanai, M., Noda, T. & Tanabe, T. (2000) *Proc. Natl. Acad. Sci. USA* **97,** 6132–6137.
34. Xu, W. & Lipscombe, D. (2001) *J. Neurosci.* **21,** 5944–5951.
35. Koschak, A., Reimer, D., Huber, I., Grabner, M., Glossmann, H., Engel, J. & Striessnig, J. (2001) *J. Biol. Chem.* **276,** 22100–22106.
36. Schorge, S., Gupta, S., Lin, Z., McEnery, M. W. & Lipscombe, D. (1999) *Nat. Neurosci.* **2,** 785–790.
37. Schiess, M. C., Asprodini, E. K., Rainnie, D. G. & Shinnick-Gallagher, P. (1993) *Brain Res.* **604,** 283–297.
38. Melliti, K., Meza, U. & Adams, B. (2000) *J. Neurosci.* **20,** 7167–7173.
39. Yu, B. & Shinnick-Gallagher, P. (1998) *J. Pharmacol. Exp. Ther.* **284,** 170–179.
40. Gelsema, A. J., McKitrick, D. J. & Calaresu, F. R. (1987) *Am. J. Physiol.* **253,** R712–R718.
41. Iwata, J., Chida, K. & LeDoux, J. E. (1987) *Brain Res.* **418,** 183–188.
42. Kapp, B. S., Gallagher, M., Underwood, M. D., McNall, C. L. & Whitehorn, D. (1982) *Brain Res.* **234,** 251–262.
43. Davis, M., Hitchcock, J. & Rosen, J. B. (1987) in *The Psychology of Learning and Motivation: Advances in Research and Theory*, ed. Bower, G. (Academic New York), pp. 263–305.
44. Hitchcock, J. & Davis, M. (1986) *Behav. Neurosci.* **100,** 11–22.
45. LeDoux, J. E. (1992) *Curr. Opin. Neurobiol.* **2,** 191–197.